Cancer Research

Affinity-Tuned ErbB2 or EGFR Chimeric Antigen Receptor T Cells Exhibit an Increased Therapeutic Index against Tumors in Mice

Xiaojun Liu[1], Shuguang Jiang[1], Chongyun Fang[1], Shiyu Yang[1], Devvora Olalere[1], Edward C. Pequignot[1], Alexandria P. Cogdill[1], Na Li[2], Melissa Ramones[2], Brian Granda[2], Li Zhou[2], Andreas Loew[2], Regina M. Young[1,3], Carl H. June[1,3,4], and Yangbing Zhao[1,3,4]

Abstract

Target-mediated toxicity is a major limitation in the development of chimeric antigen T-cell receptors (CAR) for adoptive cell therapy of solid tumors. In this study, we developed a strategy to adjust the affinities of the scFv component of CAR to discriminate tumors overexpressing the target from normal tissues that express it at physiologic levels. A CAR-expressing T-cell panel was generated with target antigen affinities varying over three orders of magnitude. High-affinity cells recognized target expressed at any level, including at levels in normal cells that were undetectable by flow cytometry. Affinity-tuned cells exhibited robust antitumor efficacy similar to high-affinity cells, but spared normal cells expressing physiologic target levels. The use of affinity-tuned scFvs offers a strategy to empower wider use of CAR T cells against validated targets widely overexpressed on solid tumors, including those considered undruggable by this approach. *Cancer Res; 75(17); 3596–607. ©2015 AACR.*

Introduction

Adoptive immunotherapy with chimeric antigen receptor (CAR)-engineered T (CART) cells can target and kill malignant cells, thereby inducing durable clinical responses in hematopoietic malignancies (1–3). However, many commonly targeted tumor antigens are also expressed by healthy tissues and on-target, off-tumor toxicity from T-cell–mediated destruction of normal tissue has limited the development of this otherwise promising type of cancer therapy. Recent reports on severe adverse events associated with treatment of cancer patients with CAR- or T-cell receptor (TCR)-engineered T lymphocytes further illustrate the critical importance of target selection for safe and efficient therapy (4–7). In specific, the targeting of ErbB2 (Her2/neu or CD340) with high affinity CARTs led to serious toxicity due to target recognition on normal cardiopulmonary tissue (8), and similarly, the presence of relatively high levels of EGFR in healthy skin leads to dose-limiting skin toxicity (9).

Selecting highly tissue-restricted antigens, cancer testis antigens, mutated gene products or viral proteins as targets could significantly improve the safety profile of using CART cells. However, none of these antigens is present with high frequency in common cancers. Most of the top-ranked target antigens that could be targeted by CART are expressed in potentially important normal tissues, such as ErbB2, EGFR, MUC1, PSMA, and GD2 (10). Current strategies for generating CARs consist of selecting scFvs with high affinity, as previous studies have shown that the activation threshold is inversely correlated with the affinity of the scFv (11, 12). However, it was found that after TCR stimulation, there is a narrow window of affinity for optimal T-cell activation, and increasing the affinity of the TCR does not necessarily improve treatment efficacy (13, 14).

Here, we have tested the hypothesis that equipping T cells with high-affinity scFv may limit the utility of CARs, due to poor discrimination of the CART for tumors and normal tissues that express the same antigen at lower levels. We sought to determine whether fine-tuning the affinity of the scFv could increase the ability of CART cells to discriminate tumors from normal tissues expressing the same antigen at lower levels. In this study, CARs with affinities against two validated targets, ErbB2 and EGFR, which are amplified or overexpressed in variety of cancers but are also expressed, at lower levels by normal tissues were tested against multiple tumor lines, as well as primary cell lines from normal tissues and organs. We found that decreasing the affinity of the scFv could significantly increase the therapeutic index of CARs, while maintaining robust antitumor efficacy both *in vitro* and in xenogeneic mouse tumor models.

Materials and Methods

Cell lines and primary human lymphocytes

SK-BR3, SK-OV3, BT-474, MCF7, MDA231, MDA468, HCC2281, MDA-361, MDA-453, HCC-1419, HCC-1569, UACC-812, LnCap,

[1]Abramson Cancer Center, University of Pennsylvania, Philadelphia, Pennsylvania. [2]Novartis Institutes for Biomedical Research, Cambridge, Massachusetts. [3]Abramson Family Cancer Research Institute, Perelman School of Medicine, University of Pennsylvania, Philadelphia, Pennsylvania. [4]Department of Pathology and Laboratory Medicine, Perelman School of Medicine, University of Pennsylvania, Philadelphia, Pennsylvania..

Note: Supplementary data for this article are available at Cancer Research Online (http://cancerres.aacrjournals.org/).

Corresponding Authors: Yangbing Zhao, Smilow Center for Translational Research, 3400 Civic Center Boulevard, Building 421, 8th Floor, Room 122, Philadelphia, PA 19104-5156. Phone: 215-746-7618; Fax: 215-573-8590; E-mail: yangbing@exchange.upenn.edu; and Carl H. June, E-mail: cjune@exchange.upenn.edu

doi: 10.1158/0008-5472.CAN-15-0159

MDA-175, MCF-10A, HCC38, and HG261 cell lines were purchased from ATCC and cultured as instructed. Primary cell lines (keratinocytes, osteoblast, renal epithelial, pulmonary artery endothelial cells, pulmonary artery smooth muscle, neural progenitor, $CD34^+$ enriched PBMC) were obtained from Promocell and cultured according to their protocols. Primary lymphocytes were isolated from normal donors provided by the University of Pennsylvania Human Immunology Core (Philadelphia, PA) and cultured in R10 medium (RPMI-1640 supplemented with 10% FCS; Invitrogen). Primary lymphocytes were stimulated with Dynabeads coated with CD3 and CD28 stimulatory antibodies (Life Technologies) as described (15). T cells were cryopreserved at day 10 in a solution of 90% FCS and 10% DMSO at 1×10^8 cells/vial.

Generation of CAR constructs for mRNA electroporation and lentiviral transduction

CAR scFv domains against ErbB2 or EGFR were synthesized and/or amplified by PCR, based on sequencing information provided by the relevant publications (16, 17), linked to CD8 transmembrane domain and 4-1BB and CD3 zeta intracellular signaling domains, and subcloned into pGEM.64A RNA-based vector (18) or pTRPE lentiviral vectors (19).

mRNA *in vitro* transcription and T-cell electroporation

T7 mscript systems kit (CellScript) was used to generate *in vitro* transcription RNA. CD3/CD28 bead stimulated T cells were electroporated with *in vitro* transcription RNA using BTX EM830 (Harvard Apparatus BTX) as previously described (18).

Flow-cytometric analysis

Antibodies were obtained from the following suppliers: anti-human CD3 (BD Biosciences, 555335), anti-human CD8 (BD Biosciences 555366), anti-human CD107a (BD Biosciences 555801), anti-human CD137 (BD Biosciences 555956). Cell surface expression of ErbB2 was detected by biotylated anti-ErbB2 Affibody (Abcam, ab31890), and EGFR by FITC-conjugated anti-EGFR affibody (Abcam, ab81872). EGFR, ErbB2, and CD19-specific CAR expressions were detected by biotin-labeled polyclonal anti-human F(ab)2 antibody for (EGFR CAR) or anti-mouse F(ab)2 antibody (for ErbB2 and CD19 CARs; Jackson Immunoresearch). Samples were then stained with phycoerythrin-labeled streptavidin (eBioscience, 17-4317-82). Flow-cytometric acquisition was performed on either a BD FacsCalibur or Accuri C6 Cytometer (BD Biosciences). Analysis was performed using FlowJo software (Treestar).

ELISA assays

Target cells were washed and suspended at 1×10^6 cells/mL in R10 medium. Of note, 100 μL each target cell type were added in triplicate to a 96-well round bottom plate (Corning). Effector T cells were washed and resuspended at 1×10^6 cells/mL in R10 medium and then 100 μL of T cells were combined with target cells in the indicated wells. The plates were incubated at 37°C for 18 to 24 hours. After the incubation, supernatant was harvested and subjected to an ELISA assay (eBioscience).

CD107a staining

Cells were plated at an E:T of 1:2 (1×10^5 effectors: 2×10^5 targets) in 160 μL of R10 medium in a 96-well plate. Of note, 20 μL of phycoerythrin-labeled anti-CD107a Ab was added and the plate was incubated at 37°C for 1 hour before adding Golgi Stop (2 μL Golgi Stop in 3 mL R10 medium, 20 μL/well; BD Biosciences, 51–2092 KZ) and incubating for another 2.5 hours. Then 5 μL FITC-anti-CD8 and 5 μL streptavidin-allophycocyanin (APC)-anti-CD3 were added and incubated at 37°C for 30 minutes. After incubation, the samples were washed with FACS buffer and analyzed by flow cytometry.

CFSE-based T-cell proliferation assay

Resting CD4 T cells were washed and suspend at concentration of 1×10^7 cells/mL in PBS. Then 120 μL CFSE working solution (25 μmol/L CFSE) was added to 1×10^7 cells for 3.5 minutes at 25°C. The labeling was stopped with 5% FBS (in PBS), washed twice with 5% FBS, and cultured in R10 with 10 IU/mL IL2. After overnight culture, the CFSE-labeled T cells were electroporated with indicated CAR RNA. Two to 4 hours after electroporation, T cells were suspended at concentration of 1×10^6/mL in R10 medium (with 10 IU/mL IL2). Tumor or K562 cell lines were irradiated and suspended at 1×10^6/mL in R10 medium. Cells were plated at an E:T of 1:1 (5×10^5 effectors: 5×10^5 targets) in 1 mL of complete RPMI medium in a 48-well plate. T cells were then counted and fed every 2 days from day 3. CFSE dilution was monitored by flow cytometry at day 3, day 5, and day 7.

Luciferase-based CTL assay

Nalm6-CBG tumor cells were generated and used in a modified version of a luciferase-based cytolytic T-cell (CTL) assay (20). Briefly, Click beetle green luciferase (CBG)-T2A-eGFP was lentivirally transduced into Nalm6 tumor cells and sorted for GFP expression. Resulting Nalm6-CBG cells were electroporated with ErbB2 RNA and resuspended at 1×10^5 cells/mL in R10 medium and incubated with different ratios of T cells (e.g., 30:1, 15:1, etc.) 8 hours at 37°C. Of note, 100 μL of the mixture was transferred to a 96-well white luminometer plate, 100 μL of substrate was added, and the luminescence was immediately determined. Results are reported as percent killing based on luciferase activity in wells with tumor, but no T cells. (% killing $= 100 - ((\text{RLU from well with effector and target cell coculture})/(\text{RLU from well with target cells}) \times 100)$).

Mouse xenograft studies

Studies were performed as previously described with certain modifications (15, 19). Briefly, 6- to 10-week old NOD-SCIDγ−/− (NSG) mice were injected subcutaneously with 1×10^6 PC3-CBG tumors cells on the right flank at day 0 and the same mice were given SK-OV3-CBG tumor cells (5×10^6 cells/mouse, s.c.) on the left flank at day 5. The mice were treated with T cells via the tail vein at day 23 post PC3-CBG tumor inoculation such that both tumors were approximately 200 mm^3 in volume. Lentivirally transduced T cells were given as indicated.

Results

Lowering the affinity of the anti-ErbB2 scFv improves the therapeutic index of ErbB2 CART cells *in vitro*

We compiled a panel of tumor lines with a wide range of ErbB2 expression as measured by flow cytometry (Fig. 1A). SK-OV3 (ovarian cancer), SK-BR3 (breast cancer), BT-474 (breast cancer) overexpress ErbB2, while EM-Meso (mesothelioma), MCF7 (breast cancer), 293T (embryonic kidney 293 cell), A549 (lung cancer), 624mel (melanoma), PC3 (prostate cancer), MDA231 (breast cancer) express ErbB2 at lower levels and ErbB2 was not detected in MDA468 (breast cancer). ErbB2 mRNA levels were

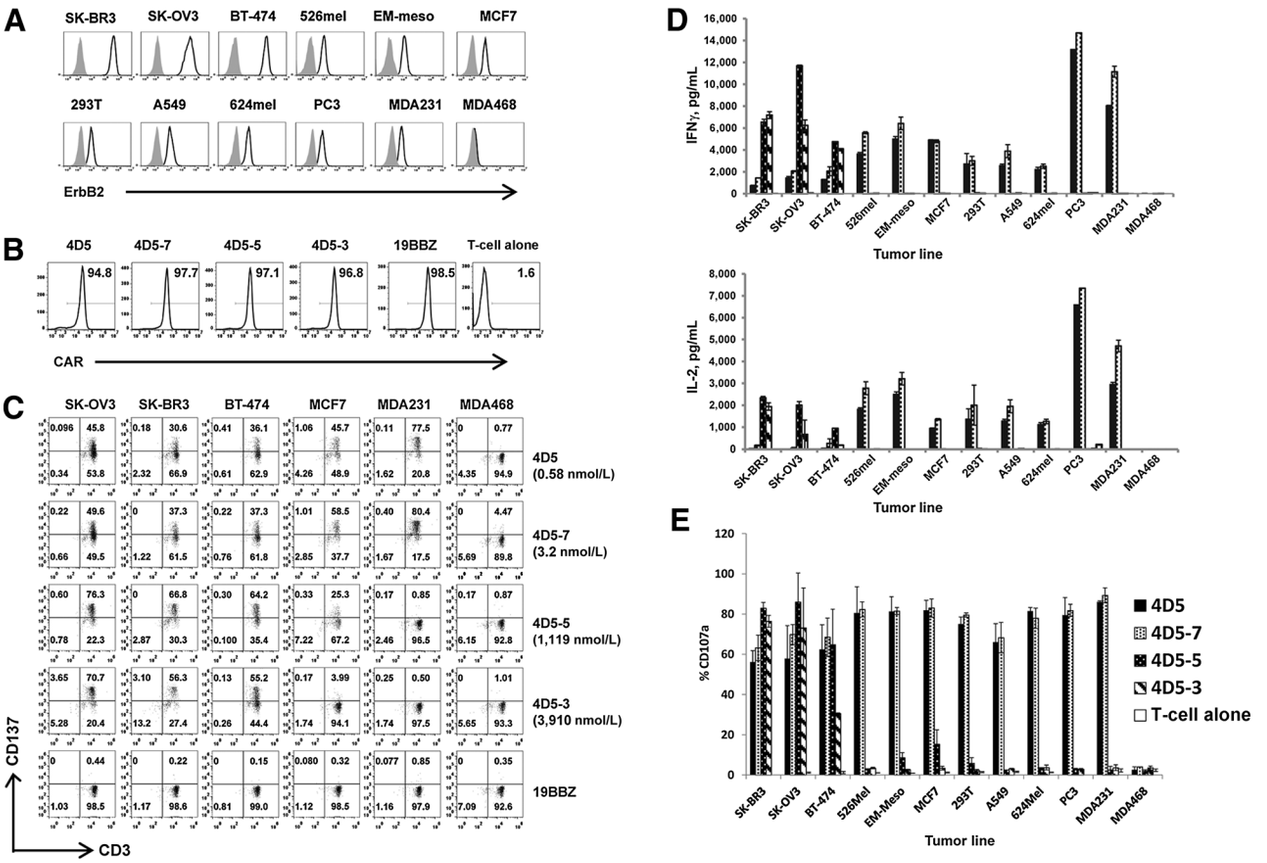

Figure 1.
Characterization of ErbB2 affinity-tuned CART cells and tumor cell lines. A, detection of ErbB2 surface expression on tumors and cell lines. Cells were stained with anti-ErbB2 Affibody-biotin and detected with APC (open histograms); cells incubated with APC alone indicate background (gray-filled histograms). B, FACS analysis of affinity-tuned CAR expression in mRNA electroporated T cells. T cells were electroporated with indicated CAR mRNA and one day after the electroporation, the CAR expression was detected using an anti-mouse IgG Fab antibody (for both CD19.BBZ and ErbB2.BBZ CARs). T cells without electroporation were used as a negative control. C, the induction of CD137 (4-1BB) expression on CART cells after stimulation by tumor cells was measured. One day after electroporation, the various CART cells (K_D, nmol/L) were cocultured with the indicated tumor cell lines. CD137 and CD3 expression was measured after 24 hours (CD3+ gated). D, cytokine secretion was measured (ELISA) in culture supernatants. T cells were electroporated with affinity-tuned ErbB2 CAR mRNA as indicated. One day after the electroporation, the CART cells were cocultured with indicated tumor cell lines for 24 hours. Bar charts show results from a representative experiment (values represent the average ± SD of triplicates) for IFNγ (top) and IL2 (bottom). E, CD107a upregulation on CART cells stimulated by tumors. T cells were electroporated with ErbB2 CAR mRNAs encoding the indicated scFv and one day later, the CART cells were cocultured with the indicated cell line for 4 hours. CD107a expression $CD3^+$ T cells was measured (values represent the average ± SD of four similar independent experiments).

also measured by real-time PCR, and there was a strong correlation between the two techniques (Supplementary Fig. S1).

A panel of ErbB2 CARs was constructed making use of scFvs derived from the published mutations of 4D5-8 antibody (4D5; ref. 16). The monovalent affinities of the ErbB2 scFvs varied by approximately three orders of magnitude (Supplementary Table S1), in contrast with the corresponding mutant antibodies that retained binding affinities within 10-fold of each other (16). CARs were constructed by linking the various scFvs to the CD8 alpha hinge and transmembrane domain followed by the 4-1BB and CD3 zeta intracellular signaling domains. The CARs were expressed by lentiviral vector technology or by cloning into an RNA-based vector (18). After production of mRNA by *in vitro* transcription and electroporation into T cells, the surface expression of the panel of affinity-modified ErbB2 RNA CARs was similar (Fig. 1B). To compare recognition thresholds, the panel of ErbB2 CART cells was stimulated with ErbB2 high-expressing (SK-BR3, SK-OV3, and BT-474) or low-expressing tumor cell lines (MCF7, 293T, A549, 624Mel, PC3, MDA231 and MDA468), and T-cell activation was assessed by upregulation of CD137 (4-1BB; Fig. 1C), secretion of IFNγ and IL2 (Fig. 1D), and induction of surface CD107a expression (Fig. 1E); the data in Supplementary Fig. S2 shows a representative experiment. T cells expressing a CD19-specific CAR or untransfected T cells served as control for allogeneic reactivity. Lower affinity CART cells (4D5-5 and 4D5-3) were strongly reactive to tumors with amplified ErbB2 expression and exhibited undetectable or low reactivity to the tumor lines that expressed ErbB2 at lower levels. In contrast, higher affinity CART cells (4D5 and 4D5-7) showed strong reactivity to tumor lines expressing high and low levels of ErbB2. These results were extended by assaying additional ErbB2-expressing cell lines (Supplementary Fig. S3). Interestingly, higher affinity CART cells secreted greater levels of IFNγ and IL2 when exposed to targets expressing low levels of ErbB2, whereas lower affinity CART cells secreted more cytokines when exposed to cells expressing high levels of target (Fig. 1D). As expected, the CD19.

BBZ CAR was not reactive against ErbB2-expressing cell lines. In summary, higher affinity 4D5.BBZ or 4D5-7.BBZ T cells recognized all the *ErbB2* expressing lines tested, whereas CARs with lower affinity scFvs, 4D5-5-BBZ or 4D5-3-BBZ, were highly reactive to all tumor lines with overexpressed ErbB2, but displayed negligible reactivity to cell lines expressing low or undetectable levels of ErbB2.

ErbB2 CARs with lower affinity scFvs discriminate between tumor cells expressing low and high levels of *ErbB2*

To exclude any tumor-specific effects that might contribute to the above results, we assayed the activity of the panel of ErbB2. BBZ CART cells against a single tumor line expressing varying levels of ErbB2. We observed that T cells expressing higher affinity scFvs (4D5 and 4D5-7) recognized K562 cells electroporated with *ErbB2* RNA at doses as low as 0.001 μg, which is 100-fold lower than the flow cytometrically detectable level of 0.1 μg mRNA (Fig. 2A and B). In contrast, the CARs with lower affinity scFvs (4D5-5 and 4D5-3) only recognized K562 electroporated *ErbB2* RNA at doses of 0.5 μg (4D5-5; Fig. 2A) or higher, indicating that CART cell sensitivity was decreased by 500- (4D5-5) to 2,000-fold (4D5-3) compared with the high-affinity 4D5 CART cells. Moreover, the antigen dose-associated reactivity observed with lower affinity ErbB2 CARs (4D5-5 and 4D5-3; Fig. 2A and B), was confirmed by performing a CFSE-based proliferation assay (Fig. 2C). Interestingly, decreasing the CAR RNA dose 5-fold

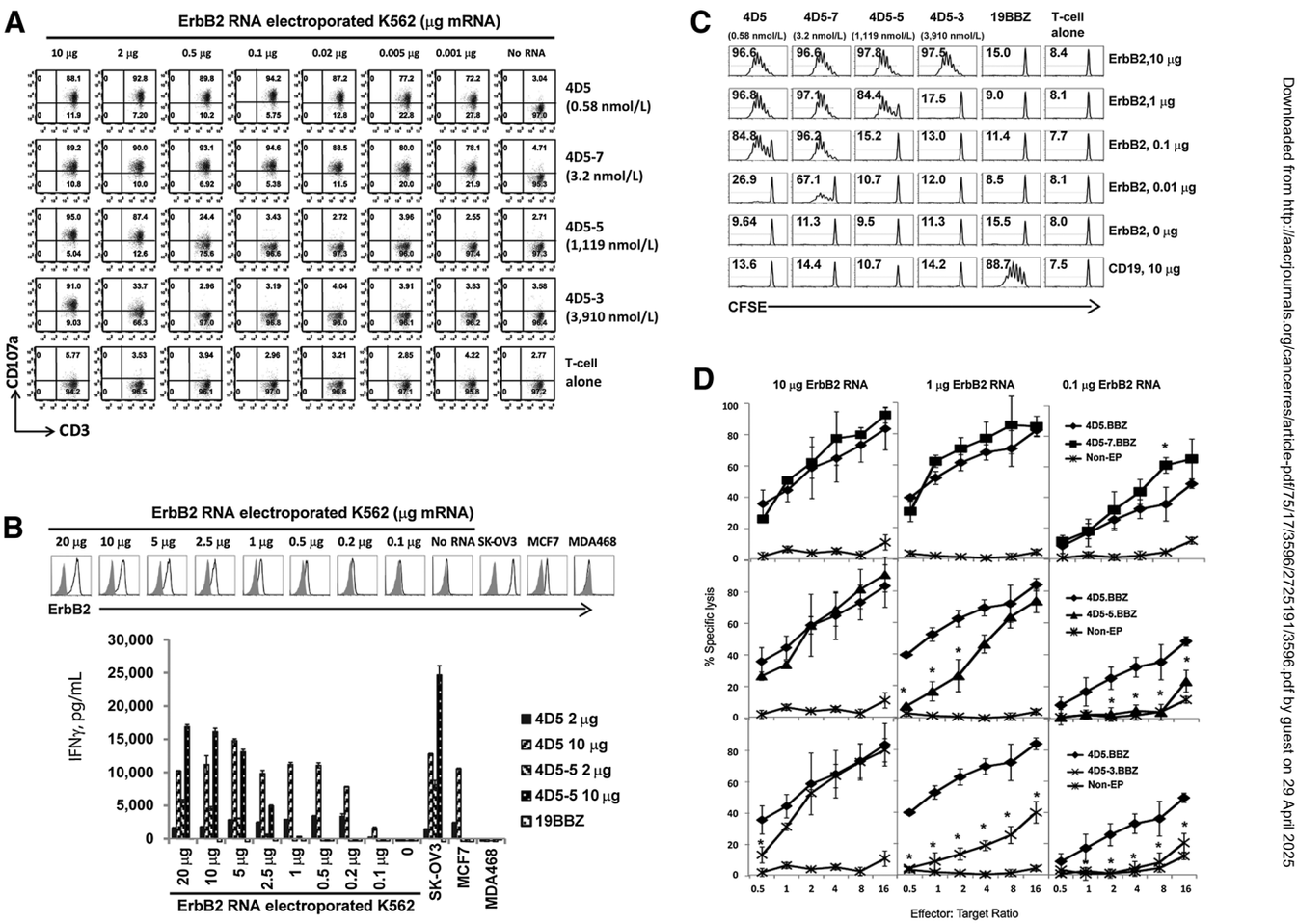

Figure 2.
Control of ErbB2 target recognition density by scFv affinity tuning. A, K562 cells were electroporated with indicated amounts of ErbB2 mRNA and CART cells expressing the indicated scFv (K_D, nmol/L) were cocultured with target for 4 hours and the percentage CD107a expression was quantified on $CD3^+$ cells. B, IFNγ secretion by the panel of ErbB2 CART cells stimulated by ErbB2 mRNA electroporated K562 cells. K562 cells were electroporated with the indicated amount of ErbB2 mRNA (top). T cells were electroporated with 2 μg or 10 μg ErbB2 CAR mRNA as indicated. CART cells were cocultured with indicated K562 targets and IFNγ secretion was measured by ELISA after 24 hours (bottom). C, proliferation of the panel of affinity-tuned CART cells after stimulation by ErbB2 mRNA electroporated K562 cells. Resting CD4 T cells were labeled with CFSE and electroporated with 10 μg CAR mRNA. K562 cells were electroporated with the indicated amount of ErbB2 mRNA or control CD19 mRNA. The T cells and irradiated targets were cultured (1:1 ratio) for 7 days and CFSE dilution was measured by flow cytometry (CD3 gated); the percentage of divided T cells is shown. D, cytolytic activity of affinity-tuned CART cells, using non-electroporated T cells (Non-EP) as control, against Nalm6-CBG ErbB2-expressing target cells was measured. T cells were electroporated with ErbB2 CAR mRNA as indicated. Nalm6-CBG (click beetle green) target cells were electroporated with ErbB2 mRNA at the indicated dose. One day after the electroporation, the CART cells were cocultured with Nalm6-CBG cells at indicated E:T ratio and percentage of specific lysis was calculated after 8 hours. All groups were compared with 4D5.BBZ. The results shown here are the averages of three independent experiments (*, $P < 0.05$, Student t test).

(from 10 μg RNA/100 μL T cells to 2 μg RNA/100 μL T cells), further increased the antigen recognition threshold of the T cells with lower affinity CARs as assessed by cytokine secretion (Fig. 2B), suggesting that fine tuning of CAR density on the surface of the T cells is also an important variable.

We used a luciferase-based CTL assay to determine whether T cells with affinity-decreased CARs could maintain potent killing activity against ErbB2 overexpressing targets while sparing cells expressing lower ErbB2 levels. When Nalm6 target cells were transfected with 10 μg ErbB2 RNA, T cells with either higher or lower affinity ErbB2 CARs effectively lysed target cells. CARs with higher affinity scFvs (4D5 and 4D5-7) exhibit potent lytic activity against target cells transfected with 1 μg *ErbB2* RNA, but lower affinity scFvs (4D5-5 and 4D5-3) showed decreased killing activity. Finally, only CARs with higher affinity scFvs were able to kill target cells expressing very low amounts of target after electroporation with 0.1 μg ErbB2 RNA (Fig. 2D). These data support that fine-tuning the affinity of ErbB2 CART cells enhances discrimination of ErbB2 overexpressing tumor from cells that have low or undetectable levels of ErbB2 expression.

Affinity-decreased ErbB2 CART cells fail to recognize physiologic levels of ErbB2

Given the previous serious adverse event that occurred upon administration of the high-affinity ErbB2 CAR that incorporated the scFv from the parental 4D5 trastuzumab antibody (8), it is of paramount importance to evaluate potential reactivity of the reduced affinity ErbB2 CART cells to physiologic levels of ErbB2 expression. To address this, six primary cell lines isolated from different organs were tested for ErbB2 expression. Most of the primary lines had detectable levels of surface ErbB2, with the neural progenitor line expressing the highest levels of target (Fig. 3A). T cells expressing the high-affinity 4D5 CAR were strongly reactive to all primary lines tested, as evidenced by levels of CD107a upregulation (Fig. 3B). However, T cells expressing the affinity decreased ErbB2 CARs 4D5-5 and 4D5-3 exhibited no reactivity to the primary lines with the exception of weak reactivity to the neural progenitor line.

Comparable effects with affinity-tuned ErbB2 CARs expressed using lentiviral transduction or RNA electroporation

To establish comparability between T cells permanently expressing CARs by lentiviral transduction with mRNA electroporated CART cells, the panel of affinity-tuned CARs was expressed in T cells from the same normal donor using either lentiviral transduction or mRNA electroporation (Fig. 4A, top). T cells were stimulated with tumor cell lines (Fig. 4A, middle), or K562 cells, expressing varying amounts of ErbB2 (Fig. 4A, bottom). CART cell recognition and activation were monitored by CD107a upregulation (Fig. 4B and C), CD137 upregulation (Supplementary Fig. S4) and IFNγ secretion (Fig. 4D and E). In agreement with the previous ErbB2 mRNA CART cell results, T cells that constitutively expressed high-affinity CARs showed strong reactivity to all cell lines expressing ErbB2; no correlation was observed between antigen expression levels and T-cell activity. In contrast, T cells with low-affinity CARs expressed by lentiviral technology demonstrated a robust correlation between target antigen expression and activation (Fig. 4B–E), similar to RNA CART cells. These results confirm that the sensitivity of ErbB2 antigen recognition is dependent on scFv affinity using both mRNA electroporated and lentiviral-transduced CART cells.

Affinity-decreased ErbB2 CART cells eliminate tumor *in vivo* and significantly reduced the toxicity against tissues expressing physiologic levels of ErbB2

To extend the above *in vitro* results, a series of experiments were conducted in NSG mice with advanced vascularized tumor xenografts. On the basis of data above in Fig. 1A, the human ovarian cancer cell line SK-OV3 was selected as a representative ErbB2 overexpressing tumor and PC3, a human prostate cancer line, was chosen to model normal tissue ErbB2 levels. We first compared the antitumor efficacy of ErbB2 CART cells expressing either the high-affinity 4D5 scFv or the low affinity 45D-5 scFv in NSG mice with day 18 established flank SK-OV3 tumors (Supplementary Fig. S5). Serial bioluminescence imaging revealed that both the high- and low-affinity CART cells resulted in the rapid elimination of the tumors.

To further evaluate the therapeutic index of the low-affinity ErbB2 CART cells *in vivo*, a mouse model was designed to simultaneously compare the efficacy and normal tissue toxicity of the high-affinity (4D5.BBZ) and low-affinity (4D5-5.BBZ) ErbB2 CARs. SK-OV3 and PC3 tumor cell lines were injected subcutaneously into opposite flanks of the same NSG mouse and T cells were administered when tumor volumes reached approximately 200 mm^3. Mice were injected (i.v.) with either 3×10^6 or 1×10^7 CART cells on day 23 and serial bioluminescence imaging and tumor size assessments were conducted. Mice treated with either dose of the CART cells exhibited nearly complete regression of the ErbB2 overexpressing SK-OV3 tumor (Fig. 5A and B). In addition, almost complete regression of the PC3 tumor expressing ErbB2 at low levels on the opposite flank was also seen for the mice treated with high-affinity 4D5-based CART cells. In contrast, the progressive tumor growth of PC3 was observed in the mice treated with low affinity 4D5-5–based CART cells, indicating that although the lower affinity CART cells were efficacious against ErbB2 overexpressing tumor, they show limited or no significant reactivity against cells expressing ErbB2 at physiologic levels. Moreover, the selective tumor elimination was observed in mice treated at both high and low doses of CART cells. The above effects were not due to allorecognation because progressive tumor growth of both tumors was observed in mice treated with mock transduced T cells.

Affinity tuning of scFv increases the therapeutic index of EGFR CART cells

To test the broader applicability the strategy to fine tune the affinity of the scFv, we evaluated a panel of EGFR CARs. EGFR.BBZ CARs were constructed from scFvs derived from the parental human anti-EGFR antibody C10 (21). The monovalent affinities of the panel of EGFR-specific scFvs varied over a range of approximately 300-fold (17). The 2224, P2-4, P3-5, and C10 scFvs were cloned into an RNA-based vector and *in vitro* transcribed for T-cell mRNA electroporation. Levels of CAR surface expression were assayed and found to be similar among the EGFR CAR constructs (Fig. 6A, top). To compare reactivities of the panel of EGFR CARs, CART cells were stimulated with EGFR-expressing tumor cell lines that have a broad range of EGFR expression at the cell surface (Fig. 6A, bottom). CART cell activation was evaluated by levels of CD107a upregulation; the data are summarized in Fig. 6B. Higher affinity EGFR CARs (2224.BBZ and P2-4.BBZ) responded to all

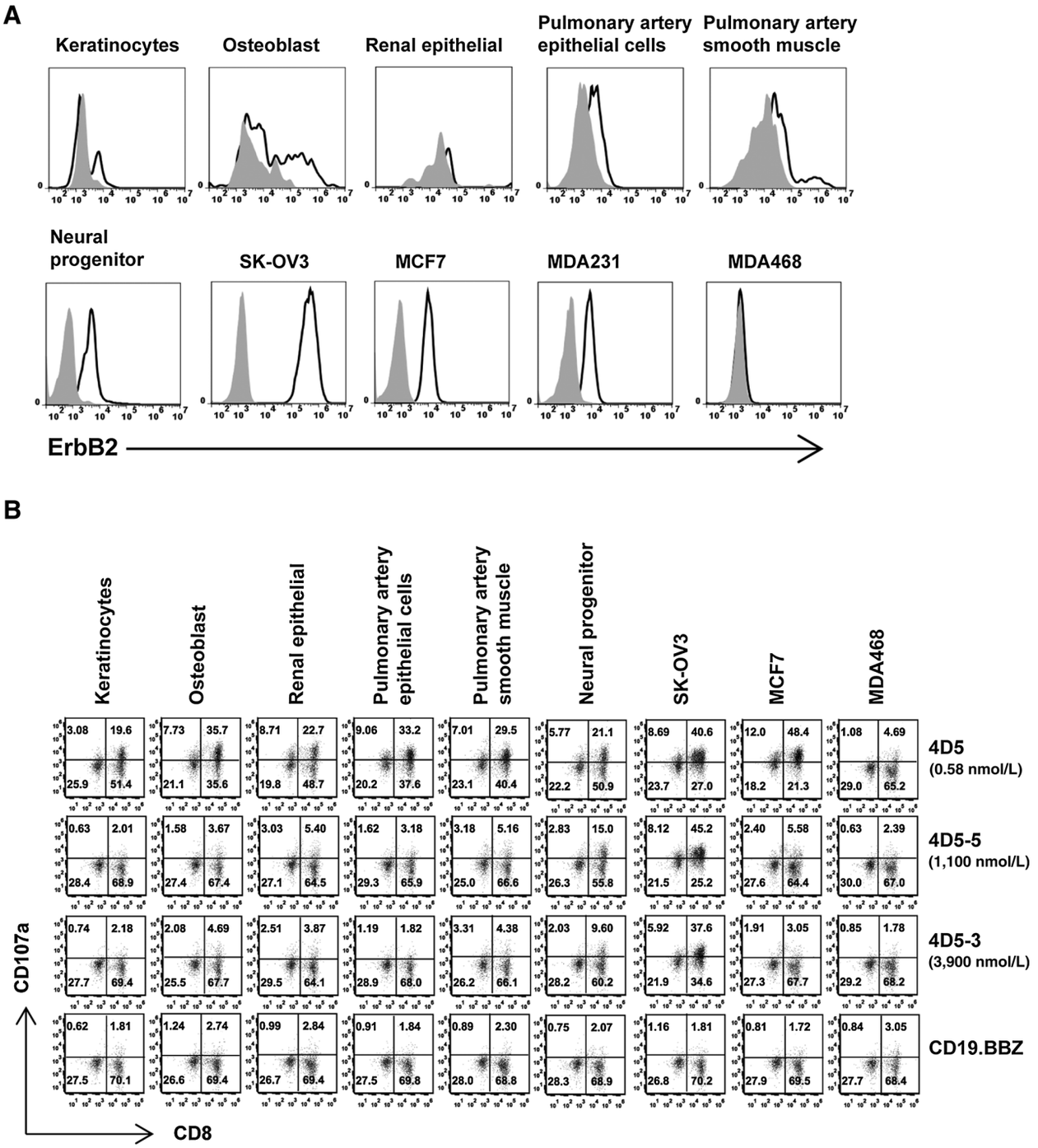

Figure 3.
Selective targeting of ErbB2 on primary cell lines. A, cell lines were stained using anti-ErBb2 Affibody-biotin and detected using APC (open histograms); cells stained with APC only were used as control (gray-filled histograms). B, the panel of CART cells was stimulated with the indicated cell line for 4 hours and the percentage of CART cells expressing CD107a was measured by gating on $CD3^+$ cells.

EGFR-positive tumor lines (MDA468, MDA231, and SK-OV3) regardless of EGFR expression levels (Fig. 6B). However, the reactivity exhibited by lower affinity EGFR CARs (P3-5.BBZ and C10.BBZ) against EGFR-expressing tumor lines correlated with the levels of EGFR expression. Furthermore, lower affinity EGFR CARs displayed more potent reactivity to the EGFR overexpressing tumor, MDA468, than the higher affinity EGFR CARs, while provoking a much weaker response to EGFR low-expressing cells (Fig. 6B). None of the EGFR CART cells reacted to the EGFR-negative tumor line K562.

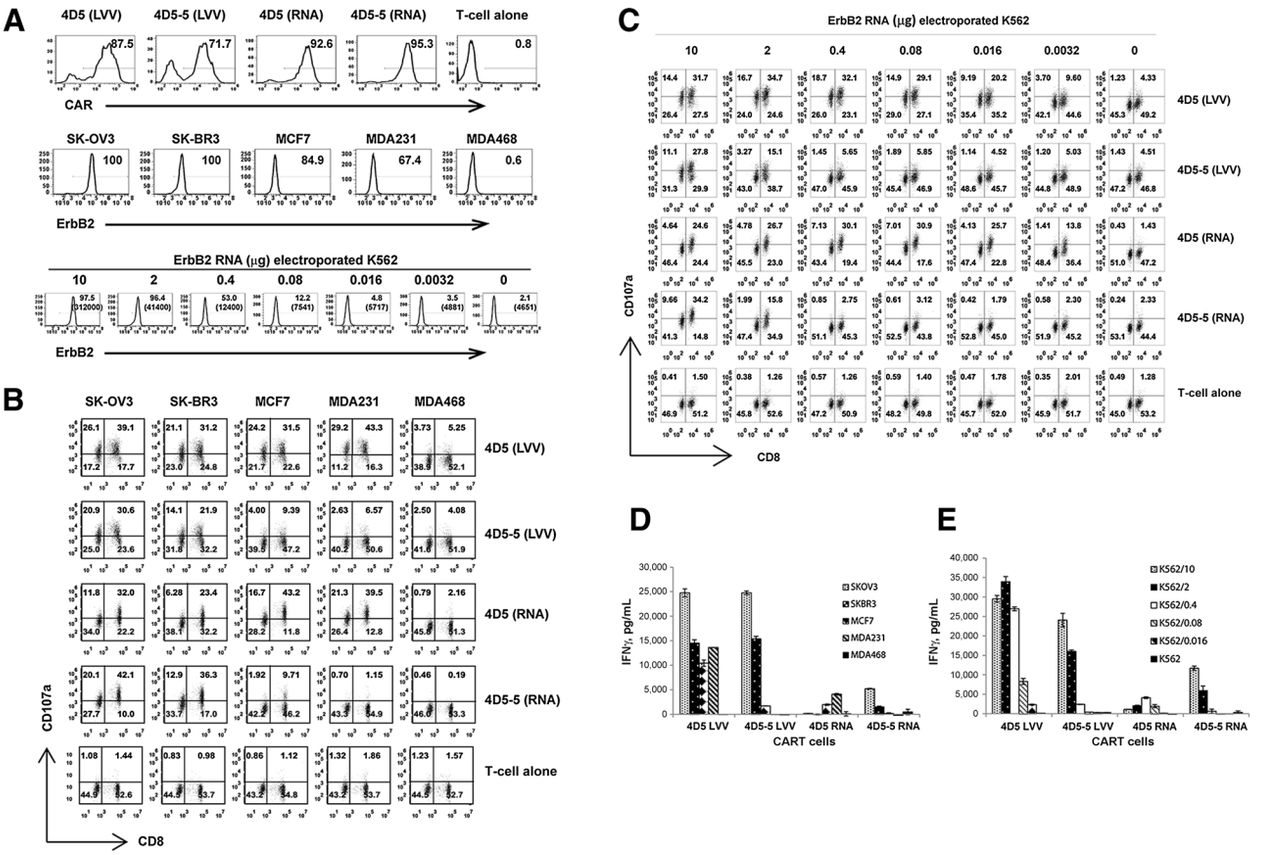

Figure 4.

Comparison of the activity of ErbB2 CART cells engineered with lentiviral vector or mRNA electroporation. A, T cells were modified with high (4D5) or low (4D5-5) affinity ErbB2 CAR using lentiviral transduction (LVV) or mRNA electroporation (RNA) as indicated. The percentage of CAR expression and brightness was measured using anti-mouse IgG Fab antibody (top). ErbB2 expression on a panel of tumor lines and K562 cells electroporated with ErbB2 mRNA was detected by flow cytometry (middle and bottom); percentage of cells with surface expression of ErB2 and mean fluorescence intensity in parenthesis are shown for K562 cells. B, CD107a upregulation was measured on lentiviral transduced or mRNA electroporated CART cells after 4-hour stimulation with indicated tumor lines (gated on $CD3^+$ cells). C, induction of CD107a expression was measured on lentiviral transduced or mRNA electroporated CART cells after 4-hour stimulation with ErbB2 electroporated K562 cells by gating on $CD3^+$ cells. D, IFNγ secretion by lentiviral transduced or RNA electroporated CART cells was measured by Elisa after 24 hours. E, IFNγ production by CART cells measured 24 hours after stimulation with K562 cells electroporated with indicated amount of ErbB2 mRNA.

To confirm that the level of response was related to scFv affinity and the level of EGFR expression, and to exclude tumor-specific effects, the panel of EGFR CART cells was cocultured with K562 cells expressing varying levels of EGFR after electroporation with mRNA (Fig. 6C). The higher affinity EGFR CARs did not discriminate between target cells with different levels of EGFR expression (Fig. 6E). For example, T cells expressing EGFR CAR 2224.BBZ responded equally well to K562 cells electroporated with a 200-fold difference in EGFR mRNA (0.1–20 μg). However, in agreement with the above ErbB2 CAR results, the lower affinity EGFR CARs (P3-5 and C10) exhibited a high correlation between T-cell responses and EGFR expression levels (Fig. 6E).

To confirm the increased safety profile of the lower affinity EGFR CARs, we tested the reactivities of EGFR CARs against primary cells derived from different organs. Five primary cell lines and five tumor cell lines were tested for both surface levels of EGFR (Fig. 6D) and ability to trigger CART cell reactivity (Fig. 6F). Three of the primary cell lines examined express detectable levels of EGFR and two did not (pulmonary artery smooth muscle and PBMC). Two of the tumor cell lines (MCF7 and Raji) did not express detectable EGFR on the cell surface. Comparing EGFR CART cells to CD19 CART cells, T cells with higher EGFR affinity CARs (2224 and P2-4) reacted to all the primary lines tested and all of the tumors except Raji (Fig. 6F). However, T cells with the affinity decreased EGFR CART cells P3-5 and C10 were not reactive to any of the five primary cells tested (Fig. 6F). CD19-specific CART cells reacted to the $CD19^+$ line Raji, and to PBMCs, presumably to the B cells in PBMC, but did not respond to any of the tumor lines or other primary cell lines. These data demonstrate that our strategy to affinity tune scFv can increase the therapeutic index for CART cells that target either ErbB2 or EGFR.

Discussion

The efficacy of CART cells is dictated in part by the differential expression of the target antigen in tumor versus normal tissue. Our results demonstrate that CARs with known severe on-target toxicities can be reengineered by affinity tuning, retaining potent *in vivo* efficacy while eliminating or reducing toxicity. In particular,

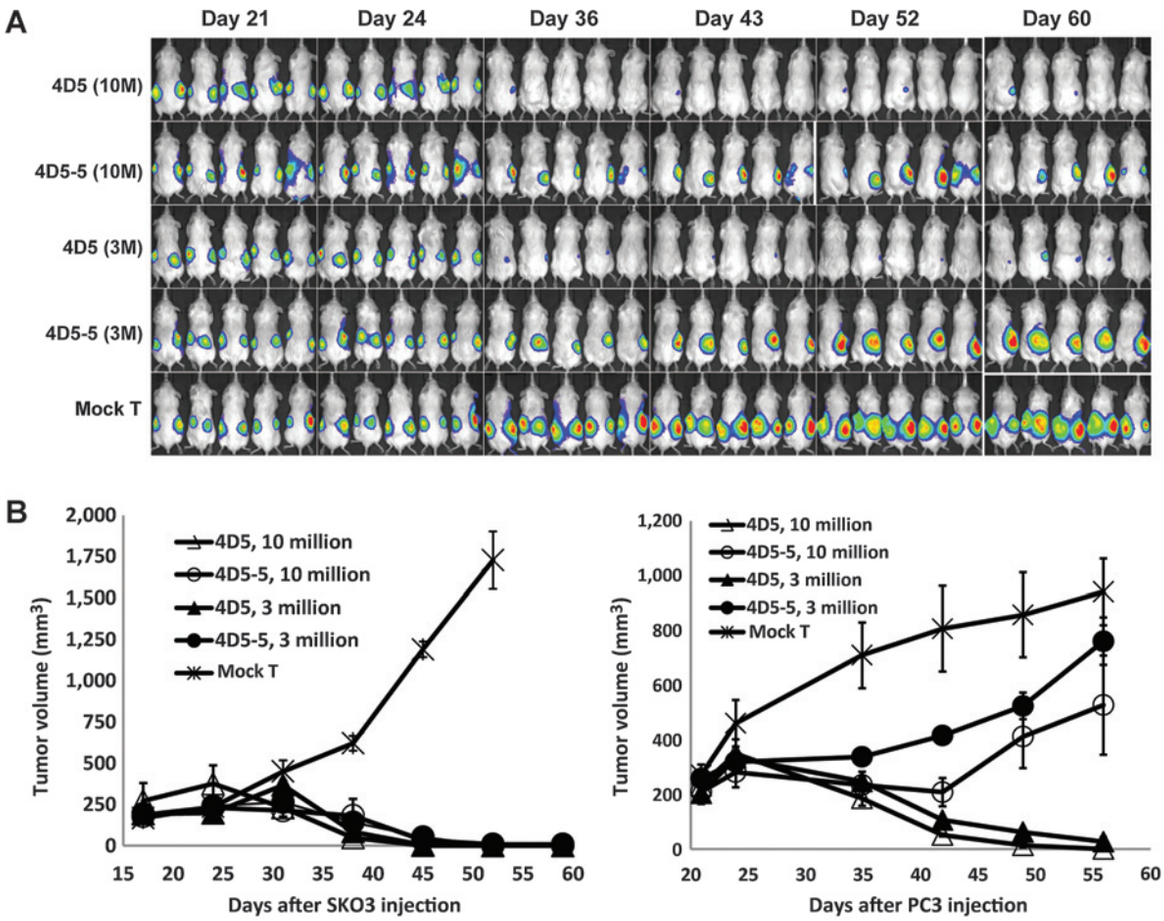

C SK-OV3 tumor size

Group#	Treatment group	Slope	P: Compared with group 5
1	4D5BBZ, 10e6	−10.87	<0.001
2	4D5-5BBZ, 10e6	−5.18	<0.001
3	4D5BBZ, 3e6	−7.46	<0.001
4	4D5-5BBZ, 3e6	−6.75	<0.001
5	T-cell alone	44.24	

PC3 tumor size

Group#	Treatment group	Slope	P: Compared with group 5	P: Compared with group 1	P: Compared with group 3
1	4D5BBZ, 10e6	−9.42	<0.001		
2	4D5-5BBZ, 10e6	7.98	0.001	<0.001	
3	4D5BBZ, 3e6	−7.54	<0.001		
4	4D5-5BBZ, 3e6	13.10	0.077		<0.001
5	T-cell alone	18.93			

Figure 5.
Affinity-tuned ErbB2 CART cells increase the therapeutic index and induce regression of advanced vascularized tumors in mice. A, *in vivo* discrimination of high ErbB2 (SK-OV3)- and low ErbB2 (PC3)-expressing tumors by affinity-tuned CARs. T cells modified with different affinity ErbB2 CARs by lentiviral transduction were tested in dual-tumor engrafted NSG mice. Mice ($n = 5$) were implanted with PC3-CBG tumor cells (1×10^6 cells/mouse, s.c.) on the right flank on day 0. On day 5, the same mice were given SK-OV3-CBG tumor cells (5×10^6 cells/mouse, s.c.) on the left flank. The mice were treated with T cells (i.v.) at day 23 after PC3 tumor inoculation. CART cells were given as a single injection of 1×10^7/mouse (10 million) or 3×10^6/mouse (3 million) as indicated. Mice treated with nontransduced T cells served as control. Animals were imaged at the indicated time post-PC3 tumor inoculation. B, SK-OV3 tumor size (left) or PC3 tumor sizes (right) in dual-tumor grafted NSG mice treated with the indicated ErbB2 CAR. Tumor sizes were measured, and the tumor volume was calculated and plotted. C, biostatistics analysis results for the tumor size. Data (not transformed) was analyzed for day ≤ 56 (PC3) or day ≤ 52 (SKOV3). Method was mixed models, with day, group, and day $\times$ group interaction as fixed effects, and mouse as random effect. For random effect, each mouse had a separate intercept and slope (method also known as random coefficients). *P* values presented are interaction *P* values.

the 4D5 CAR based on trastuzumab had lethal toxicity (8), due to recognition of physiologic levels of ErbB2 expressed in cardiopulmonary tissues (22). Here, we demonstrate that by reducing the affinity of scFv used in CART cells by 2- to 3-log, a substantial improvement in the therapeutic index was seen for ErbB2 and EGFR CART cells. CART cells with lower affinity scFv showed equally robust antitumor activity against ErbB2 overexpressing tumors as compared with the high-affinity CARs, but displayed significantly reduced reactivity against physiologic levels of ErbB2.

CARs specific for the B-cell lineage antigens CD19 and CD20 have been tested by a variety of groups and have displayed potent efficacy in B-cell malignancies (23). However in solid tumors, with the exception of tumor-specific isoforms such as EGFRviii (24), on target toxicity is anticipated to be a severe limitation for CART cells. This limitation is expected to be more serious with

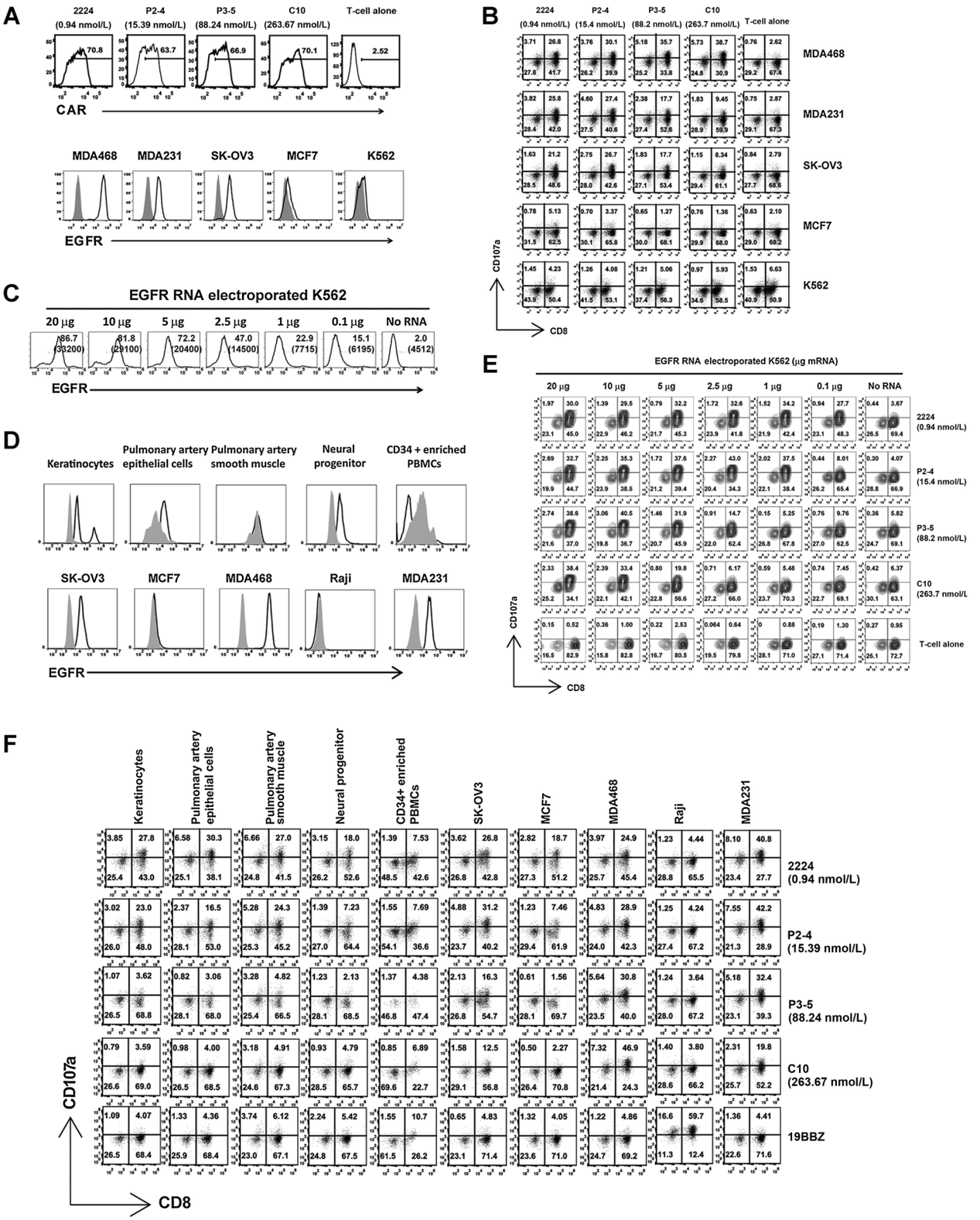

Figure 6.
Characterization of EGFR affinity-tuned CART cells and tumor cell lines. A, CAR expression on T cells electroporated with EGFR CAR mRNA were stained by an anti-human IgG Fab and detected by flow cytometry staining (top); the affinity of the scFv is indicated (nmol/L). Tumor lines (bottom) were stained with anti-EGFR Affibody-FITC (open histograms); the same cells were stained with mouse IgG1-FITC as isotype control (gray-filled histograms). (*Continued on the following page.*)

CARs than with antibody therapies using intact antibodies or antibody drug conjugates, due to the lower limit of target sensitivity for CART cells compared with antibody-based therapies that differ by several orders of magnitude. Our present studies using target cells electroporated with ErbB2 or EGFR mRNA are consistent with previous studies indicating that CART cells can recognize tumor cells with approximately 100 targets per cell (25). In contrast, amplification of *ErbB2* occurs in approximately 20% to 25% of primary human breast cancers and typically results in overexpression of ErbB2 protein at >1 million copies per cell (26, 27). At present, available data indicate that cancer cells do not lose ErbB2 expression when they become refractory to ErbB2-directed therapies (28).

Our findings support previous work from Chmielewski (11), suggesting that the high-affinity CARs exhibit less discrimination between target cells with high or low target expression levels. However, the present results differ from Chmielewski and coworkers; in that none of the higher affinity CARs (with K_D ranging from 15 to 16 nmol/L) in their report were reactive to cells with low-level expression of *ErbB2* and their lower affinity CAR that only recognized tumors with amplified *ErbB2* showed a substantial reduction in T-cell efficacy compared with the higher affinity CARs. In contrast, we found that the ErbB2 CAR using the 4D5 scFv with K_D at 0.3 nmol/L was strongly reactive to keratinocytes and even to cell lines transfected with extremely low amounts ErbB2 mRNA that were 100 times below detectable levels, while affinity-tuned CART cells retained reactivity to ErbB2 amplified tumors that was at least as potent as the high-affinity CAR, both *in vitro* and in aggressive mouse tumor models. Some variables that may explain these differences include the use of different scFvs (C5.6 vs. 4D5) that may recognize different epitopes, distinct CAR signaling domain configuration (zeta alone vs. 4-1BB-zeta), and different gene transfer approaches (retroviral transduction versus RNA electroporation or lentiviral transduction) that may affect CAR surface expression levels on the T cells. Together, this suggests that each of these factors should be considered when selecting the affinity of a CAR in relevant clinical situations.

The advent of more potent adoptive transfer strategies has prompted a reassessment of targets previously considered as safe using weaker immunotherapeutic strategies (29). Strategies to maximize the therapeutic index of CART cells include target selection, CAR design, cell manufacturing, and gene transfer techniques. In addition to affinity tuning, other strategies being developed to manage on target toxicity include the use of dual CART cell approaches (30, 31), conditional deletion and suicide systems (32, 33), and repeated infusions of T cells having mRNA CARs that have transient expression and self-limiting toxicity (34).

Efficient T-cell activation by pMHC on the surface of APCs requires an optimal dwell time of TCR–pMHC interaction that is sufficiently long to complete the signal cascade, but also short enough to permit serial engagement of multiple TCR molecules by pMHC, especially when pMHC density is low (35, 36). Increasing TCR affinity above "natural" affinity range (1–100 μmol/L) could reduce the ability to recognize low-density pMHC (37–39). The reactivity of high-affinity TCRs against low-density cognate pMHC could be rescued by decreasing MHC expression (39), or decreasing TCR–pMHC interaction by using mutated MHC molecules (35) or stimulating with plate-bound pMHC molecules (38). These findings suggest that the activation of T cells with very high-affinity TCR is not only determined by the density of pMHC on the APCs, but the interaction of TCR with MHC and the presence of endogenous pMHC profoundly impact T-cell activation as well. CAR imitates TCR by using TCR/CD3 zeta signaling moiety to activate T cells. However, CART cells are largely different from conventional alpha/beta T cells by the facts that (i) CART recognizes antigen independent of target MHC and CD8 expression; (ii) CART activates through only zeta chain without involvement of gamma, delta, and epsilon chains; and (iii) costimulator signal is incorporated in CART. Despite the differences between CART and conventional T cells, our finding that decreasing the affinity of a CAR to "natural" high-affinity range (1–10 μmol/L) increased CART activities against antigen high expression target is consistent with the finding for conventional T cells whose optimal activation requires TCR affinity in the "natural"affinity range. As mentioned above, decreasing overall avidity of TCR/pMHC led to improved serial engagement of TCR against low-density pMHC for high-affinity TCR. Similarly, we found in our current study that high-affinity CART cells showed improved activities against low levels of target antigen, which presumably is caused by decreased binding half-life of CAR/antigen interaction and improved serial engagement due to overall decreased avidity. Therefore, the signals that T cells receive from high-affinity CAR against low enough surface antigen might be the same as that from lower affinity CAR against high surface antigen.

There are several limitations of our study that will require evaluation in a phase I pilot trial. This includes the cell to cell variation in expression of ErbB2 and EFGR (40), and the unknown variation that may occur in the setting of inflammation. In addition, although we have demonstrated that affinity-tuning can increase the therapeutic index for ErbB2 and EGFR, it remains unknown whether this is a general strategy. In addition to scFv affinity, other variables that require examination on a case by case basis include the location of the target epitope, the length of the hinge, and the nature of the signaling domain (12, 41).

In summary, ErbB2 and EGFR have previously been considered as undruggable targets for CART cells. Given that dysregulation of the expression of ErbB2 and EGFR occurs frequently in multiple human carcinomas, including breast, glioblastoma,

(*Continued.*) B, EGFR CAR recognition sensitivity is correlated with affinity. A panel of EGFR CART cells with the indicated affinity of the scFv (K_D, nmol/L) was stimulated with the panel of tumors expressing EGFR at the density shown in A. After 4-hour stimulation, CD107a upregulation on the CART cells was detected by gating on $CD3^+$ cells. C, K562 cells were electroporated with the indicated amount of EGFR mRNA and EGFR expression was detected using anti-EGFR Affibody-FITC staining 14 hours post-electroporation. D, EGFR expression on a panel of primary cell lines and tumor lines was measured by FACS using anti-EGFR Affibody-FITC (open histograms), with the same cells stained with mouse IgG1-FITC as isotype control (gray-filled histograms). E, EGFR CAR recognition sensitivity is correlated with affinity. T cells were electroporated with the panel of EGFR CARs with different affinities as indicated and stimulated with K562 electroporated with EGFR mRNA at different levels as shown in D. After 4-hour stimulation, CD107a expression on CART cells was measured by gating on $CD3^+$ cells. F, affinity-dependent recognition of primary cell lines and tumor cells using affinity-tuned EGFR CARs. T cells were electroporated with the indicated EGFR CAR mRNA. One day after electroporation, the CART cells were stimulated with the panel of cells for 4 hours and the induction CD107a expression on the CART cells was quantified ($CD3^+$ gated).

lung, pancreatic, ovarian, head and neck squamous cell cancer, and colon cancer, our findings have considerable clinical importance. Our strategy has the potential not only to improve the safety profile and clinical outcome of CARs directed against validated targets, but also to expand the landscape to targets not previously druggable with CART cells because of on-target toxicities. More generally, our findings suggest that safer and more potent CARs can be designed by using affinity-tuned scFvs for a variety of common carcinomas.

Disclosure of Potential Conflicts of Interest

X. Liu reports receiving commercial research grant from Novartis and has ownership interest in a patent in cell and gene therapy licensed to Novartis. A. Loew has ownership interest (including patents) in Novartis. C.H. June reports receiving commercial research grant from Novartis and has ownership interest in patents owned by University of Pennsylvania and licensed to Novartis. Y. Zhao reports receiving commercial research grant from Novartis and has ownership interest in patents in the field of cell and gene therapy licensed to Novartis. No potential conflicts of interest were disclosed by the other authors..

Authors' Contributions

Conception and design: X. Liu, A. Loew, C.H. June, Y. Zhao
Development of methodology: X. Liu, D. Olalere, A. Loew, Y. Zhao
Acquisition of data (provided animals, acquired and managed patients, provided facilities, etc.): X. Liu, S. Jiang, C. Fang, D. Olalere, A.P. Cogdill, N. Li, M. Ramones, B. Granda, L. Zhou, A. Loew, Y. Zhao
Analysis and interpretation of data (e.g., statistical analysis, biostatistics, computational analysis): X. Liu, S. Jiang, C. Fang, D. Olalere, E.C. Pequignot, M. Ramones, B. Granda, L. Zhou, A. Loew, R.M. Young, Y. Zhao
Writing, review, and/or revision of the manuscript: X. Liu, B. Granda, A. Loew, R.M. Young, C.H. June, Y. Zhao
Administrative, technical, or material support (i.e., reporting or organizing data, constructing databases): S. Yang, D. Olalere, A.P. Cogdill

Acknowledgments

The authors thank their colleagues at Novartis J Brogdon, P. Gotwals, S. Ettenberg, and W. Sellers for insightful discussions and L. Johnson for primary cell lines.

Data and Materials Availability

Data and materials are available from the authors under a material transfer agreement.

Grant Support

This work was supported in part by grants from the NIH (P01CA066726 and 2R01CA120409) and by Novartis.

The costs of publication of this article were defrayed in part by the payment of page charges. This article must therefore be hereby marked *advertisement* in accordance with 18 U.S.C. Section 1734 solely to indicate this fact.

Received January 20, 2015; revised May 14, 2015; accepted May 14, 2015; published online September 1, 2015.

References

1. Kochenderfer JN, Wilson WH, Janik JE, Dudley ME, Stetler-Stevenson M, Feldman SA, et al. Eradication of B-lineage cells and regression of lymphoma in a patient treated with autologous T cells genetically engineered to recognize CD19. Blood 2010;116:4099–102.
2. Porter DL, Levine BL, Kalos M, Bagg A, June CH. Chimeric antigen receptor-modified T cells in chronic lymphoid leukemia. N Engl J Med 2011; 365:725–33.
3. Brentjens RJ, Davila ML, Riviere I, Park J, Wang X, Cowell LG, et al. CD19-targeted T cells rapidly induce molecular remissions in adults with chemotherapy-refractory acute lymphoblastic leukemia. Sci Transl Med 2013;5:177ra138.
4. Lamers CH, Sleijfer S, Vulto AG, Kruit WH, Kliffen M, Debets R, et al. Treatment of metastatic renal cell carcinoma with autologous T-lymphocytes genetically retargeted against carbonic anhydrase IX: first clinical experience. J Clin Oncol 2006;24:e20–2.
5. Parkhurst MR, Yang JC, Langan RC, Dudley ME, Nathan DA, Feldman SA, et al. T cells targeting carcinoembryonic antigen can mediate regression of metastatic colorectal cancer but induce severe transient colitis. Mol Ther 2011;19:620–6.
6. Morgan RA, Chinnasamy N, Abate-Daga D, Gros A, Robbins PF, Zheng Z, et al. Cancer regression and neurological toxicity following anti-MAGE-A3 TCR gene therapy. J Immunother 2013;36:133–51.
7. Linette GP, Stadtmauer EA, Maus MV, Rapoport AP, Levine BL, Emery L, et al. Cardiovascular toxicity and titin cross-reactivity of affinity enhanced T cells in myeloma and melanoma. Blood 2013;122:863–71.
8. Morgan R, Yang J, Kitano M, Dudley M, Laurencot C, Rosenberg S. Case report of a serious adverse event following the administration of T cells transduced with a chimeric antigen receptor recognizing ERBB2. Mol Ther 2010;18:843–51.
9. Perez-Soler R, Saltz L. Cutaneous adverse effects with Her1/EGFR-targeted agents: Is there a silver lining? J Clin Oncol 2005;23:5235–46.
10. Cheever MA, Allison JP, Ferris AS, Finn OJ, Hastings BM, Hecht TT, et al. The prioritization of cancer antigens: a national cancer institute pilot project for the acceleration of translational research. Clin Cancer Res 2009;15: 5323–37.
11. Chmielewski M, Hombach A, Heuser C, Adams GP, Abken H. T cell activation by antibody-like immunoreceptors: increase in affinity of the single-chain fragment domain above threshold does not increase T cell activation against antigen-positive target cells but decreases selectivity. J Immunol 2004;173:7647–53.
12. Hudecek M, Lupo-Stanghellini MT, Kosasih PL, Sommermeyer D, Jensen MC, Rader C, et al. Receptor affinity and extracellular domain modifications affect tumor recognition by ROR1-specific chimeric antigen receptor T cells. Clin Cancer Res 2013;19:3153–64.
13. Zhong S, Malecek K, Johnson LA, Yu Z, Vega-Saenz de Miera E, Darvishian F, et al. T-cell receptor affinity and avidity defines antitumor response and autoimmunity in T-cell immunotherapy. Proc Natl Acad Sci U S A 2013; 110:6973–8.
14. Schmid DA, Irving MB, Posevitz V, Hebeisen M, Posevitz-Fejfar A, Sarria JC, et al. Evidence for a TCR affinity threshold delimiting maximal CD8 T cell function. J Immunol 2010;184:4936–46.
15. Barrett DM, Zhao Y, Liu X, Jiang S, Carpenito C, Kalos M, et al. Treatment of advanced leukemia in mice with mRNA engineered T cells. Hum Gene Ther 2011;22:1575–86.
16. Carter P, Presta L, Gorman CM, Ridgway JB, Henner D, Wong WL, et al. Humanization of an anti-p185HER2 antibody for human cancer therapy. Proc Natl Acad Sci U S A 1992;89:4285–9.
17. Zhou Y, Drummond DC, Zou H, Hayes ME, Adams GP, Kirpotin DB, et al. Impact of single-chain Fv antibody fragment affinity on nanoparticle targeting of epidermal growth factor receptor-expressing tumor cells. J Mol Biol 2007;371:934–47.
18. Zhao Y, Moon E, Carpenito C, Paulos CM, Liu X, Brennan AL, et al. Multiple injections of electroporated autologous T cells expressing a chimeric antigen receptor mediate regression of human disseminated tumor. Cancer Res 2010;70:9053–61.
19. Carpenito C, Milone MC, Hassan R, Simonet JC, Lakhal M, Suhoski MM, et al. Control of large, established tumor xenografts with genetically retargeted human T cells containing CD28 and CD137 domains. Proc Natl Acad Sci U S A 2009;106:3360–5.
20. Moon EK, Wang LC, Dolfi DV, Wilson CB, Ranganathan R, Sun J, et al. Multifactorial T-cell hypofunction that is reversible can limit the efficacy of chimeric antigen receptor-transduced human T cells in solid tumors. Clin Cancer Res 2014;20:4262–73.
21. Heitner T, Moor A, Garrison JL, Marks C, Hasan T, Marks JD. Selection of cell binding and internalizing epidermal growth factor receptor antibodies from a phage display library. J Immunol Methods 2001;248:17–30.

22. Press MF, Cordon-Cardo C, Slamon DJ. Expression of the HER-2/neu proto-oncogene in normal human adult and fetal tissues. Oncogene 1990;5:953–62.
23. Maus MV, Grupp SA, Porter DL, June CH. Antibody modified T cells: CARs take the front seat for hematologic malignancies. Blood 2014;123:2625–35.
24. Morgan RA, Johnson LA, Davis J, Zheng Z, Woolard K, Reap EA, et al. Recognition of glioma stem cells by genetically modified T cells targeting EGFRvIII and development of adoptive cell therapy for glioma. Hum Gene Ther 2012;23:1043–53.
25. Stone JD, Aggen DH, Schietinger A, Schreiber H, Kranz DM. A sensitivity scale for targeting T cells with chimeric antigen receptors (CARs) and bispecific T-cell Engagers (BiTEs). Oncoimmunology 2012;1:863–73.
26. Robertson KW, Reeves JR, Smith G, Keith WN, Ozanne BW, Cooke TG, et al. Quantitative estimation of epidermal growth factor receptor and c-erbB-2 in human breast cancer. Cancer Res 1996;56:3823–30.
27. Vogel CL, Cobleigh MA, Tripathy D, Gutheil JC, Harris LN, Fehrenbacher L, et al. Efficacy and safety of trastuzumab as a single agent in first-line treatment of HER2-overexpressing metastatic breast cancer. J Clin Oncol 2002;20:719–26.
28. Ritter CA, Perez-Torres M, Rinehart C, Guix M, Dugger T, Engelman JA, et al. Human breast cancer cells selected for resistance to trastuzumab *in vivo* overexpress epidermal growth factor receptor and ErbB ligands and remain dependent on the ErbB receptor network. Clin Cancer Res 2007;13:4909–19.
29. Hinrichs CS, Restifo NP. Reassessing target antigens for adoptive T-cell therapy. Nat Biotechnol 2013;31:999–1008.
30. Kloss CC, Condomines M, Cartellieri M, Bachmann M, Sadelain M. Combinatorial antigen recognition with balanced signaling promotes selective tumor eradication by engineered T cells. Nat Biotechnol 2013;31:71–5.
31. Lanitis E, Poussin M, Klattenhoff AW, Song D, Sandaltzopoulos R, June CH, et al. Chimeric antigen receptor T cells with dissociated signaling domains exhibit focused anti-tumor activity with reduced potential for toxicity. Cancer Immunol Res 2013;1:43–53.
32. Di Stasi A, Tey SK, Dotti G, Fujita Y, Kennedy-Nasser A, Martinez C, et al. Inducible apoptosis as a safety switch for adoptive cell therapy. N Engl J Med 2011;365:1673–83.
33. Wang X, Chang WC, Wong CW, Colcher D, Sherman M, Ostberg JR, et al. A transgene-encoded cell surface polypeptide for selection, *in vivo* tracking, and ablation of engineered cells. Blood 2011;118:1255–63.
34. Beatty GL, Haas AR, Maus MV, Torigian DA, Soulen MC, Plesa G, et al. Mesothelin-specific chimeric antigen receptor mRNA-engineered T cells induce anti-tumor activity in solid malignancies. Cancer Immunol Res 2014;2:112–20.
35. Kalergis AM, Boucheron N, Doucey MA, Palmieri E, Goyarts EC, Vegh Z, et al. Efficient T cell activation requires an optimal dwell-time of interaction between the TCR and the pMHC complex. Nat Immunol 2001;2:229–34.
36. Valitutti S. The serial engagement model 17 years after: from TCR triggering to immunotherapy. Front Immunol 2012;3:272.
37. Thomas S, Xue SA, Bangham CR, Jakobsen BK, Morris EC, Stauss HJ. Human T cells expressing affinity-matured TCR display accelerated responses but fail to recognize low density of MHC-peptide antigen. Blood 2011;118:319–29.
38. Gonzalez PA, Carreno LJ, Coombs D, Mora JE, Palmieri E, Goldstein B, et al. T cell receptor binding kinetics required for T cell activation depend on the density of cognate ligand on the antigen-presenting cell. Proc Natl Acad Sci U S A 2005;102:4824–9.
39. Zhao Y, Bennett AD, Zheng Z, Wang QJ, Robbins PF, Yu LY, et al. High-affinity TCRs generated by phage display provide CD4+ T cells with the ability to recognize and kill tumor cell lines. J Immunol 2007;179:5845–54.
40. Szöllösi J, Balázs M, Feuerstein BG, Benz CC, Waldman FM. ERBB-2 (HER2/neu) gene copy number, p185HER-2 overexpression, and intratumor heterogeneity in human breast cancer. Cancer Res 1995;55:5400–7.
41. Guedan S, Chen X, Madar A, Carpenito C, McGettigan SE, Frigault MJ, et al. ICOS-based chimeric antigen receptors program bipolar TH17/TH1 cells. Blood 2014;124:1070–80.